第33卷 第4期 焊 接 学 报 Vol. 33 No. 4
2012年4月 TRANSACTIONS OF THE CHINA WELDING INSTITUTION April 2012

焊接工艺对 TP304 钢焊缝金属组织及性能的影响

李海涛， 杨文杰， 王 军， 尹 柯
（佳木斯大学 材料科学与工程学院，佳木斯 154007）

摘 要： 针对 TP304 不锈钢，采用三种不同的焊接工艺方法，选取合适的焊接工艺参数，成功制备三组完整的焊接接头. 通过 X 荧光化学成分分析、显微组织观察和显微硬度试验研究了不同焊接方法对 TP304 不锈钢焊缝金属组织和性能的影响. 结果表明，不同焊接方法下焊缝合金成分有所差异，且分布不均；各焊层显微组织形态和晶粒大小差异较大；整个接头的硬度值分布并不均匀，焊缝高于热影响区，热影响区高于母材. 三种焊接方法相比，TIG-MAG 焊缝的硬度值最大，TIG-SMAW 的最小. 对于薄板不锈钢焊接，TIG-MAG 组合焊法优选.

关键词： TP304 钢；焊接工艺；焊缝金属；X 荧光；显微硬度
中图分类号： TG441.3 **文献标识码：** A **文章编号：** 0253－360X(2012)04－0089－04

李海涛

0 序 言

TP304 钢是不锈钢的主体钢种，其奥氏体结构赋予了它良好的冷热加工性能、耐腐蚀性、低温性能、无磁性，及焊接性，但在焊接过程中由于热输入不断增加，奥氏体晶粒易于粗大，热影响区敏化温度范围变宽，从而导致焊接接头耐腐蚀性能降低，焊接接头容易产生热裂纹[1,2]. 奥氏体不锈钢的热导率小和线膨胀系数大，在局部加热和冷却条件下，如果焊接接头在高温停留时间较长，焊缝金属凝固过程中存在较大应力和应变，很容易在焊缝中产生凝固裂纹；另一方面，奥氏体易形成方向性很强的柱状晶焊缝组织，使得有害杂质在高温时易发生偏析和聚集，促使形成晶间液态间层，从而使焊缝中产生裂纹[3]. 因此采用合理的焊接工艺，对提高焊缝金属耐腐蚀性以及避免焊接裂纹的产生具有重要意义.

1 试验方法

试验材料为 TP304 奥氏体不锈钢，经日本岛津公司 XRF-1800 荧光光谱仪测试，其化学成分如表 1 所示，测试条件见表 2（光栅：3.0 mm，气氛：真空）. 为了便于焊接，得到成形质量较好的焊接接头，焊接前对试件开 60° V 形坡口，并对焊口两侧清理，严防漆、锈、油污等杂物的影响[4,5].

表 1 TP304 钢化学成分（质量分数，%）
Table 1 Chemical compositions of TP304 steel

Mn	Si	Cr	Ni	S，P	Fe
0.950	0.510	18.850	8.210	≤0.03	余量

表 2 荧光光谱试验条件
Table 2 Measurement conditions of X-ray fluorescence spectrum test

元素通道	靶材	管电压 U_X/kV	管电流 I_X/mA	狭缝	测试晶体	探测器	测试角度 θ/(°)	测试时间 t/s	扫描速度 v_s/(rad·min^{-1})	步长 l
S	Rh	40	95	标准	Ge	FPC	108～114	45	0.14	0.1
P	Rh	40	95	标准	Ge	FPC	138～144	45	0.14	0.1
Si	Rh	40	95	标准	PET	FPC	106～112	45	0.14	0.1
Ti-U	Rh	40	95	标准	LiF	SC	10～90	240	0.174	0.1

采用三种焊接方法，分别为 TIG-MAG，TIG-TIG，TIG-SMAW. TIG 焊采用的保护气体为纯氩，焊接时它既不与金属起化学反应也不溶解于液态金属

收稿日期：2011－03－04
基金项目：佳木斯大学校级科研资助项目(L2010-148)

中,故可以避免焊缝中金属元素的烧损和由此带来的其它焊接缺陷,故三种方法均采用 TIG 焊打底(铈钨极直径为 3.2 mm)采用 MAG 焊、TIG 焊和 SMAW 盖面. 具体焊接参数和焊接材料如表 3 所示. 填丝氩弧焊选用直流正接,自动送丝 MAG 焊选用直流反接.

表 3 焊接参数和焊接材料

Table 3 Welding parameters and solder

序号	焊接方法	焊接电流 I/A	电弧电压 U/V	焊接速度 v/(cm·s^{-1})	焊接材料	焊材直径 ϕ/mm	气体流量 q/(L·min^{-1})
1	TIG	90	14	10	18Ni9	2.5	9
	MAG	120	21	5	ER50-6	1.2	15
2	TIG	90	14	10	18Ni9	2.5	9
	TIG	110	15	11	18Ni9	2.5	9
3	TIG	90	14	10	18Ni9	2.5	9
	SMAW	120	28	18	J422	3.2	—

2 试验结果及分析

2.1 X 射线荧光试验

线切割截取焊缝,将其截面打平后采用 XRF-1800 型荧光光谱仪,试验条件同表 1 所示(将铜、钼也选为测试对象[6]),合金元素分析结果如表 4 所示.

由表 4 可见,焊缝中有 Mo,Cu 两种元素存在,尽管在母材的成分中 Mo,Cu 元素没有被列出,但在进一步的分析中始终能发现这两种元素微量存在. 各方法下焊缝合金成分差异较大,且分布不均,但都以锰,硅为一组,铬,镍为一组,铜,钼为一组呈下述规律:打底层中,锰,硅含量属 TIG-MAG 最大,TIG-TIG 最小,铬,镍含量属 TIG-TIG 最大,TIG-SMAW 最小,铜,钼含量 TIG-TIG 最大,TIG-MAG 最小;盖面层中,锰,硅含量属 TIG-MAG 最大(同打底层),TIG-SMAW 最小,铬,镍含量属 TIG-TIG 最大(同打底层),TIG-MAG 最小,铜,钼含量 TIG-TIG 最大(同打底层),TIG-SMAW 最小. 这些合金元素在焊缝中分布的差异必然导致各焊接方法下焊缝组织和力学性能的不同.

表 4 焊缝金属荧光试验结果(质量分数,%)

Table 4 Results of X-ray fluorescence spectrum

序号	焊接方法	位置	Mn	Si	S	P	Cr	Ni	Cu	Mo
1	TIG-MAG	打底	1.100	1.060	0.060	0.045	18.875	8.148	0.1536	0.095
		盖面	0.987	2.385	0.052	0.030	8.760	4.000	0.230	0.068
2	TIG-TIG	打底	0.790	0.600	0.035	0.065	18.930	8.550	0.265	0.145
		盖面	0.898	1.278	0.050	0.057	18.275	8.385	0.235	0.145
3	TIG-SMAW	打底	0.980	0.747	0.090	0.055	16.455	7.551	0.200	0.124
		盖面	0.620	1.277	0.070	0.077	8.976	4.500	0.116	0.060

2.2 显微组织观察

切取小块金相试样,打磨抛光后,经 4% 的 HNO_3 酒精溶液腐蚀处理,在奥林巴斯显微镜下观察母材及三种焊接方法下的组织形貌,如图 1 ~ 图 4 所示.

金相观察显示,母材微观组织为单一的奥氏体;TIG-MAG 底层焊缝组织为 γ + 少量 δ 相组织,盖面焊层为 γ + 析出相,小颗粒状析出相主要是富铜相,呈弥散分布;TIG-TIG 底层焊缝组成为奥氏体,呈较为粗大的柱状晶形态,盖面焊缝组织为典型的胞状

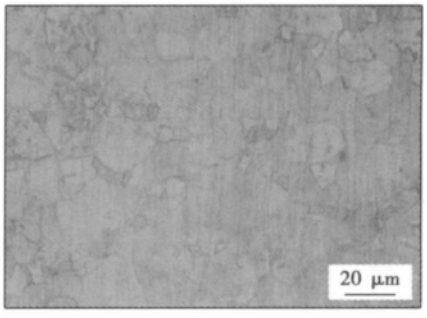

图 1 母材金相组织形貌

Fig. 1 Microstructure of base metal

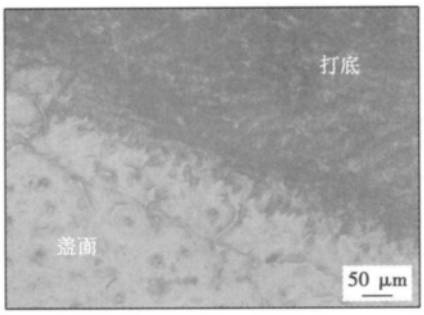

图 2　1 号焊缝金相组织形貌

Fig. 2　Microstructure of weld of No. 1

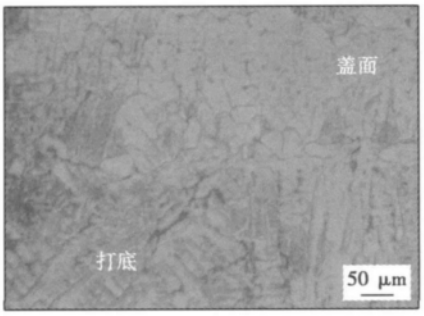

图 3　2 号焊缝金相组织形貌

Fig. 3　Microstructure of weld of No. 2

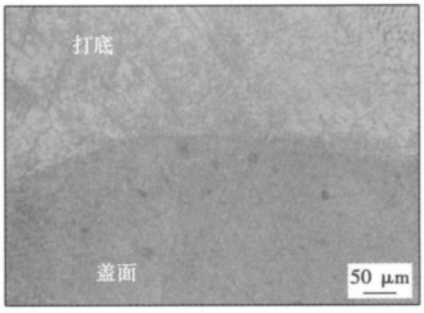

图 4　3 号焊缝金相组织形貌

Fig. 4　Microstructure of weld of No. 3

树枝晶,且伴有组织较细小的析出相; TIG-SMAW 打底层组织为较均匀的等轴晶和柱状晶,晶粒较细小,盖面焊层组织为 $\gamma+\delta$ 相.

分析以上各工艺下焊缝组织的形成,认为是焊缝金属的凝固依赖于合金成分和热力学条件. 根据 Fe-Cr-Ni 相图的浓度截面图可知,当 Cr-Ni 的比例达到 2∶1 后,开始从液态合金中析出一次 δ 铁素体,因为焊接时冷却速度快,当铬含量小于 20% 时,$\gamma\rightarrow\delta$ 转变和 δ 相析出被完全抑制,所以 TIG-MAG 底层焊缝金属的组织是奥氏体和少量残留的铁素体. 根据 Savage 理论,冷却速度和母材晶粒方向对结晶形态、结晶方向有影响,较快的冷却速度促进柱状晶的形成,中等冷却速度促进树枝晶的产生[7],各焊接方法下的冷却速度不同,必然导致组织形态差异. 由于熔池底部冷却速度较大,促进了柱状晶的生长. 此外奥氏体钢的线膨胀系数小、导热性差、焊缝熔池中金属冷却速度小、散热慢、温度梯度小、晶粒长大速度快,这也导致了粗大柱状晶的形成.

2.3　显微硬度试验

采用 HXD-1000TMC 硬度计,试验力为 1 N,保持时间为 5 s,测得母材硬度为 156 HV0.1,焊缝及 HAZ 的硬度值见表 5 和图 5.

表 5　显微硬度试验结果(HV0.1)

Table 5　Results of micro-hardness test

序号	位置	硬度值			平均值
1	打底	283	252	332.6	289.2
	盖面	367.25	343.43	413	374.56
	HAZ	166	156.7	193	171.9
2	打底	173.1	175.2	160.4	169.57
	盖面	220.3	217	200	212.43
	HAZ	166	176	162.8	168.27
3	打底	154.7	166.2	160.2	160.37
	盖面	226.1	210.2	216.1	217.47
	HAZ	155.6	170.1	165.7	163.8

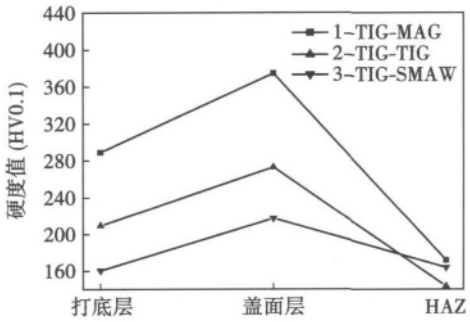

图 5　三种焊接方法不同位置硬度值

Fig. 5　Micro-hardness of three welding methods at different positions

从表 5 和图 5 可见,整个接头的硬度值分布并不均匀,焊缝高于 HAZ,HAZ 高于母材. 三种焊接方法相比,TIG-MAG 焊缝的硬度值最大,TIG-SMAW 的最小. 焊缝金属硬度高于母材和 HAZ 是由于部分母材和焊材中的合金元素在高温电弧作用下会固溶于焊缝而产生固溶强化效果,使焊缝硬度最高. 而 HAZ 由于处于半熔融状态,伴随着凝固过程的进行会有相析出,引起 HAZ 产生沉淀强化,故其硬度相对母材较高.

TIG-SMAW 方法热效率高($\eta=0.8$),焊缝组织

迅速升温，提高铬的扩散速度，不会在晶界处形成贫铬区，降低碳化物形成. 热效率高、热循环峰值温度高，高温停留时间较长，γ 晶粒易长大，导致焊后组织粗大及析出相数量减少，这些因素均致使 TIG-SMAW 方法焊缝硬度值较低. 而 TIG-MAG 焊接方法的焊缝组织析出相较多，析出强化效果明显，硬度较高. 此外从表 4 的数据可见，TIG-MAG 盖面熔敷金属中镍含量最低，镍含量的减少会提高碳在奥氏体不锈钢中的溶解度，从而使碳化物析出倾向大. 锰是奥氏体化形成元素，焊缝中锰含量的增加，主要是形成高熔点的 MnS，降低熔敷金属杂质元素(表 4 可见 TIG-MAG 方法的 Mn 元素含量最高)，这些都导致 TIG-MAG 焊缝硬度值较大.

3 结 论

(1) 焊缝中 Mo，Cu 两种元素微量存在，各方法的焊缝合金成分差异较大，且分布不均.

(2) 母材微观组织为奥氏体，TIG-MAG 底层焊缝组织为 γ + 少量 δ 相，盖面焊层为 γ + 析出相; TIG-TIG 底层焊缝为粗大的柱状晶形态，盖面焊缝组织为胞状树枝晶; TIG-SMAW 打底层组织为均匀的等轴晶和柱状晶，盖面焊层组织为 $\gamma+\delta$ 相.

(3) 硬度值分布不均匀，焊缝最高，母材最低; TIG-MAG 焊缝的硬度值最大，TIG-SMAW 的最小.

(4) 对于较薄不锈钢板，优选 TIG-MAG 组合焊接工艺.

参考文献:

[1] 王希靖，叶结和，孙丙岩，等. 0Cr18Ni9 不锈钢搅拌摩擦焊接头的微观组织和性能 [J]. 热加工工艺，2006，35(23)：36 - 38.
Wang Xijing，Ye Jiehe，Sun Bingyan，*et al*. Microstructure and mechanical properties of friction stir weld joint of 0Cr18Ni9 stainless steel [J]. Hot Working Technology Institution，2006，35(23)：36 - 38.

[2] 徐 峰. 0Cr18Ni9 不锈钢储能焊接头微观组织分析 [J]. 热加工工艺，2009，38(3)：114 - 115.
Xu Feng. Microstructure of welded joint of 0Cr18Ni9 stainless steel by capacitor discharge welding [J]. Hot Working Technology Institution，2009，38(3)：114 - 115.

[3] 芮福才. 奥氏体不锈钢与铁素体钢的焊接性能分析研究 [J]. 黑龙江电力，2002(8)：270 - 272.
Rui Fucai. Weldability analysis for austenitic steel and ferritic steel [J]. Heilongjiang Electric Power，2002(8)：270 - 272.

[4] 李海涛，陈芙蓉，胡艳华，等. 焊接热循环峰值温度对 10CrMo910 钢硬度的影响 [J]. 焊接学报，2009，30(2)：75 - 78.
Li Haitao，Chen Furong，Hu Yanhua，*et al*. Effects of peak temperature of welding thermal circle on hardness of 10CrMo910 [J]. Transactions of the China Welding Institution，2009，30(2)：75 - 78.

[5] 李海涛，陈芙蓉，胡艳华，等. 热输入对 10CrMo910 钢焊缝金属根焊层热循环的影响 [J]. 焊接学报，2011，32(1)：49 - 51.
Li Haitao，Chen Furong，Hu Yanhua，*et al*. Effects of heat input of root layer on thermal circle of 10CrMo910 [J]. Transactions of the China Welding Institution，2011，32(1)：49 - 51.

[6] 李新梅. Super304H 奥氏体钢焊接接头组织与性能研究 [D]. 济南：山东大学，2010.

[7] 孙晓娜，雷 毅，张 鹰. 厚板奥氏体不锈钢焊缝显微组织分析 [J]. 金属热处理，2006，31(10)：21 - 23.
Sun Xiaona，Lei Yi，Zhang Ying. Microstructure analysis of weld joint for austenitic stainless steel thick plate [J]. Heat Treatment of Metal，2006，31(10)：21 - 23.

作者简介: 李海涛，男，1982 年出生，硕士. 主要从事焊接热循环及焊接工艺方法方面的研究. 发表论文 7 篇. Email: Haitao0204@126.com

number of needle-like and thread-like tin whiskers were formed on the surface of the oxidized RE phases. It was noteworthy to mention that these tin whiskers kept the constant cross section during growth process. However, besides these regular tin whiskers, some new ones with special morphology, such as lapped whiskers, branch and combination of whiskers, were also found.

Key words: rare earth phase; aging; tin whisker; morphology

Fracture toughness of square drill pipe joint by narrow gap welding MA Caixia[1], ZHANG Se[2], HUANG Xusheng[2], LIN Chengxiao[1], MA Fubao[2], YANG Siqian[1] (1. Shanxi Key Laboratory of Friction Welding Technologies, Northwestern Polytechnical University, Xi'an 710072, China; 2. Shanxi Northfenglei Industrial Group Co., Ltd., Houma 043013, China). pp 77 - 80

Abstract: The test and calculation methods for the dynamic fracture toughness of 40CrMnMo square drill pipe joint produced by narrow gap pulsed metal arc welding were studied. Combined with the use of square drill pipe, pipe size and welding characteristics, the repeated impact 3-point bending test was used to test the fracture toughness of the square drill pipe joint. The crack depth was measured by using a microscope. and K_{Id} values were calculated with a FORTRAN program. The experimental results show that K_{Id} of the weld is 96% of that of the base material, but K_{Id} of the fusion line is only 89% of that of the base material. The analyses on the fracture surface and cross-sectional microstructure indicate that the bulky Widmanstatten structure near the fusion line is the main reason for a lower K_{Id}.

Key words: square drill pipe; narrow gap pulsed gas shielded metal arc welding; fracture toughness

Laser tailor welding of aluminum alloy sheet and cup axon formability of TWB LI Yuntao[1,2], ZHANG Wenjun[1], YANG Lijun[3], ZHANG Jian[1,2] (1. School of Materials Science Engineering, Tianjin University of Technology, Tianjin 300384, China; 2. Tianjin Key Laboratory for Photoelectric Materials Devices, Tianjin 300384, China; 3. School of Materials Science Engineering, Tianjin University, Tianjin 300072, China). pp 81 - 84

Abstract: The process and forming performance of laser tailor-welded board (TWB) of 6061 aluminum alloy were studied. The forming characteristics of TWB in the cup axon trials and the influence of welded beam on overall plastic forming of tailor-welded plate were analyzed. The cupping test results of laser TWB shows that the cracking generally appears in the narrow HAZ. The cupping index of TWB was slightly lower than that of base metal. During the numerical simulation process of cupping test with DYNAFORM software, only the location of the welded beam was considered but its type was ignored, and the results showed that the simulation cracking of the TWB easily occurred at the welded seam below the cupping head with the influence of the welded seam, and the simulation results were slightly different from the practical tests, which was possibly related to the set of the welded seam.

Key words: 6061 aluminum alloy sheet; laser tailor-welded; cup axon formability; DYNAFORM simulation

Establishment of cold cracking susceptibility criterion for X80 pipeline steel LI Yajuan[1,2], JIA Peng[1], LI Wushen[2], XIE Qi[2] (1. College of Science, Civil Aviation University of China, Tianjin 300300, China; 2. School of Materials Science and Engineering, Tianjin University, Tianjin 300072, China). pp 85 - 88

Abstract: The influence of welding heat input, preheat temperature and the deposited metal diffusible hydrogen content were considered, the HAZ critical stress of X80 pipeline steel was tested by implant test based on the orthogonal regression design. The significant factors on the critical stress were obtained by analysis of variance. By multiple linear regression, the critical stress equation and the cold cracking susceptibility criterion were established. The critical stress equation was analyzed. It was concluded that the initial diffusing hydrogen content had great influence on cold cracking susceptibility of X80 pipeline steel. When the initial diffusing hydrogen content is lower, the microstructure is found to be the most important factor on the critical stress. When the initial diffusing hydrogen content is higher, the residual hydrogen content has great influence on the critical stress as well as the microstructure.

Key words: pipeline steel; critical stress; cold cracking; range analysis

Study of microstructure and properties in weld metal of TP304 steel under three processes LI Haitao, YANG Wenjie, WANG Jun, YIN Ke (School of Materials Science and Engineering, Jiamusi University, Jiamusi 154007, China). pp 89 - 92

Abstract: Using three different welding processes, the appropriate welding process parameters were selected and three groups welded joints of TP304 stainless steel were prepared successfully. The microstructure and properties in weld metal zone of TP304 stainless steel under different welding methods were studied by X-fluorescent chemical composition analysis, microstructure observations and micro-hardness test. The results show that alloy composition of weld metal are different and distribute uniformly with different welding methods, microstructure morphology and grain size of the solder layer are quite different. Hardness of the joint is not evenly distribute, weld metal is higher than HAZ, and HAZ is higher than the base metal. Hardness of the weld under TIG-MAG process is maximum and TIG-SMAW process is minimum by comparing three methods. TIG-MAG welding method is better for the thin stainless steel.

Key words: TP304 steel; welding procedure; weld metal; X-ray fluorescence; micro hardness

Numerical analysis on crack tip opening displacement of strength mismatched welded joint XIONG Linyu, ZHANG Yanhua (School of Mechanical Engineering and Automation, Beihang University, Beijing 100191, China). pp 93 - 96

Abstract: Elastic-plastic behaviors of strength mismatched welded joints with cracks were investigated with finite element method. Effects of strength mismatching, crack length and stress-strain curve form of base metal on crack tip opening displacement were analyzed. The results show that the crack driving force increases with the increasing of strength mismatch